

The reconstruction of inflationary potentials

Jianmang Lin,^{1*} Qing Gao,^{2,1†} and Yungui Gong,^{1‡}

¹*School of Physics, Huazhong University of Science and Technology, Wuhan 430074, China*

²*School of Physical Science and Technology, Southwest University, Chongqing 400715, China*

17 October 2018

ABSTRACT

The observational data on the anisotropy of the cosmic microwave background constrains the scalar spectral tilt n_s and the tensor to scalar ratio r which depend on the first and second derivatives of the inflaton potential. The information can be used to reconstruct the inflaton potential in the polynomial form up to some orders. However, for some classes of potentials, n_s and r behave as $n_s(N)$ and $r(N)$ universally in terms of the number of e-folds N . The universal behaviour of $n_s(N)$ can be used to reconstruct a class of inflaton potentials. By parametrizing one of the parameters $n_s(N)$, $\epsilon(N)$ and $\phi(N)$, and fitting the parameters in the models to the observational data, we obtain the constraints on the parameters and reconstruct the classes of the inflationary models which include the chaotic inflation, T-model, hilltop inflation, s-dual inflation, natural inflation and R^2 inflation.

Key words: cosmology: inflation.

1 INTRODUCTION

The quantum fluctuation during inflation seeds the large-scale structure and imprints the information of early Universe in the anisotropies of the cosmic microwave background (CMBR). For the slow-roll inflation with a single scalar field, the scalar (Mukhanov & Chibisov 1981) and tensor (Starobinsky 1979) power spectra can be parametrized by the slow-roll parameters (Stewart & Lyth 1993). In particular, the scalar spectral tilt n_s , the amplitude of the scalar spectrum A_s and the tensor to scalar ratio r can be constrained by the observational data on CMBR. For an inflationary model, we can calculate the slow-roll parameters and the observables n_s and r , and compare the results with the observations. However, there are lots of inflationary models with different potentials (Martin et al. 2014a) and it is not an easy task to compare all the models and constrain the model parameters in the models, although we may use Bayesian evidence to select best models (Martin et al. 2014b). Recently, the temperature and polarization measurements on the CMBR by the Planck survey gave the results $n_s = 0.9645 \pm 0.0049$ (68% CL), $\ln(10^{10} A_s) = 3.094 \pm 0.034$ (68% CL) and $r_{0.002} < 0.11$ (95% CL) (Planck Collaboration I 2015; Planck Collaboration XX 2015). If we take the number of e-folds before the end of inflation at the horizon exit $N = 60$, then the measured scalar spectral

tilt can be approximated as $n_s - 1 \approx -2/N$, and r can be described as $r \sim N^{-p}$ with $p \geq 1$. The small value of r alleviates the problem imposed by the Lyth bound (Choudhury & Mazumdar 2014b; Gao et al. 2014; Choudhury 2015; Gao et al. 2015). Since the running of the scalar spectral index is a second-order effect, it is expected to be in the order of 10^{-3} for slow-roll inflationary models (Gao & Gong 2014). The running of the scalar spectral index is constrained to be $dn_s/d \ln k = -0.0057 \pm 0.0071$ (68% CL) (Planck Collaboration XX 2015).

For chaotic inflation with the power-law potential $V(\phi) = V_0 \phi^p$ (Linde 1983), we get $n_s - 1 = -(p + 2)/(2N)$ with N being the number of e-folds before the end of inflation at the horizon exit. For the hilltop models with the potential $V(\phi) = V_0(1 - \mu\phi^p)$ (Boubekeur & Lyth 2005), we get $n_s - 1 = -2(p - 1)/[(p - 2)N]$ and $r \sim 0$. For the Starobinsky model (Starobinsky 1980), we get $n_s - 1 = -2/N$ and $r = 12/N^2$. For a class of inflationary models with non-minimal coupling to gravity (Kalosh et al. 2014), it was found that $n_s - 1 = -2/N$ and $r = 12/N^2$. For natural inflation (Freese et al. 1990), we get $n_s - 1 = -[1 + \exp(-N/f^2)]/[f^2 - f^2 \exp(-N/f^2)]$ and $r = 8 \exp(-N/f^2)/[f^2 - f^2 \exp(-N/f^2)]$. Therefore, there are some universal behaviours for n_s and r which are consistent with the observations for a large class of inflationary models. The suggested simple relation between n_s and N tells us that it will be more easier to compare the models with the observational data if the slow-roll parameters and the observable n_s can be expressed in terms of N . By parametrizing the slow-roll parameter ϵ as $\epsilon = \beta/(N + 1)^\alpha$, Mukhanov derived the correspond-

* 563939360@qq.com

† gaoqing01good@163.com

‡ yggong@mail.hust.edu.cn

ing inflaton potential (Mukhanov 2013). For the simple inverse power-law form N^{-p} , Roset divided some inflationary models into two universal classes with the same $1/N$ behaviour for n_s and different power-law behaviour for r (Roest 2014). More complicated forms of $\epsilon(N)$ were also proposed by Garcia-Bellido and Roset (Garcia-Bellido & Roest 2014). The parameters α and β in the parametrization were fitted to the observational data in (Barranco et al. 2014). The consequences of the two fixed points on n_s and r in the parametrization were discussed in (Boubekeur et al. 2015). In addition to the parametrization of ϵ , the reconstruction of the inflaton potential from the parametrization of n_s with $n_s - 1 = -\alpha/N$, and from the assumption between the amplitude of the power spectrum $-\ln \Delta_R^2$ and $n_s - 1$ were also considered (Chiba 2015; Creminelli et al. 2015; Gobetti et al. 2015). On the other hand, the reconstruction of the inflaton potential from the power spectra by the method of functional reconstruction were usually applied (Hodges & Blumenthal 1990; Copeland et al. 1993; Liddle & Turner 1994; Lidsey et al. 1997; Peiris & Easther 2006; Norena et al. 2012; Choudhury & Mazumdar 2014a; Ma & Wang 2014; Myrzakulov et al. 2015; Choudhury 2016).

In this paper, we discuss the reconstruction of the inflaton potential from the parametrizations of $\epsilon(N)$, $\phi(N)$ and $n_s(N)$. The parameters in the models are fitted to the Planck temperature and polarization data. The paper is organized as follows. In the Section 2, we review the general relations between $\epsilon(N)$, $\phi(N)$, $n_s(N)$ and $V(N)$ by applying the slow-roll formula. The reconstruction of the inflaton potential from $n_s(N)$ is presented in Section 3. The reconstruction of the inflaton potential from $\epsilon(N)$ is presented in Section 4. The reconstruction of the inflaton potential from $\phi(N)$ is presented in Section 5. The conclusions are drawn in Section 6.

2 GENERAL RELATIONS

For the single slow-roll inflation, to the first order of approximation, we have

$$n_s - 1 \approx 2\eta - 6\epsilon, \quad r = 16\epsilon. \quad (1)$$

Since

$$\frac{d \ln \epsilon}{dN} = 2\eta - 4\epsilon, \quad (2)$$

so

$$n_s - 1 = -2\epsilon + \frac{d \ln \epsilon}{dN}. \quad (3)$$

If we parametrize the slow-roll parameter ϵ as a function of the number of e-folds before the end of inflation, then we can derive the parametrization $n_s(N)$ and $r(N)$. Conversely, if we parametrize $n_s(N)$, we can solve equation (3) to get $\epsilon(N)$, and then $r(N)$.

From the energy conservation of the scalar field, we have

$$d \ln \rho_\phi + 3(1 + w_\phi) d \ln a = 0. \quad (4)$$

Since $\rho_\phi \approx V(\phi)$, $d \ln a = -dN$, and

$$1 + w_\phi = \frac{\dot{\phi}^2}{\rho_\phi} \approx \frac{\dot{\phi}^2}{V(\phi)} \approx \frac{2}{3}\epsilon, \quad (5)$$

so

$$\epsilon \approx \frac{1}{2} \frac{d \ln V}{dN} = \frac{1}{2} (\ln V)_{,N} > 0, \quad (6)$$

and the inflaton always rolls down the potential during inflation. Substituting the above result into equation (3), we get (Chiba 2015)

$$n_s - 1 \approx -(\ln V)_{,N} + \left(\ln \frac{V_{,N}}{V} \right)_{,N} = \left(\ln \frac{V_{,N}}{V^2} \right)_{,N}. \quad (7)$$

If we have any one of the functions $\epsilon(N)$, $n_s(N)$ and $V(N)$, we can derive the other functions by using equations (3), (6) and (7).

To derive the form of the potential $V(\phi)$, we need to find the functional relationship $\phi(N)$ for the scalar field. Note that

$$d\phi = \pm \sqrt{2\epsilon(N)} dN, \quad (8)$$

where the sign \pm depend on the sign of the first derivative of the potential and the scalar field is normalized by the Planck mass $M_{pl} = (8\pi G)^{-1/2} = 1$, so

$$\phi - \phi_e = \pm \int_0^N \sqrt{2\epsilon(N)} dN. \quad (9)$$

Once one of the functions $\epsilon(N)$, $n_s(N)$, $\phi(N)$ and $V(N)$ is known, in principle we can derive n_s , r and the potential $V(\phi)$ by using the relations (3), (6), (7) and (8).

Before we present particular parametrizations, we briefly discuss the effect of second-order corrections. To the second-order of approximation, we have (Stewart & Lyth 1993; Schwarz et al. 2001)

$$n_s - 1 \approx 2\eta - 6\epsilon - \left(\frac{10}{3} + 24C \right) \epsilon^2 + \frac{2}{3} \eta^2 + (16C - 2)\epsilon\eta + \left(\frac{2}{3} - 2C \right) \xi, \quad (10)$$

$$r \approx 16\epsilon \left[1 + \left(4C - \frac{4}{3} \right) \epsilon + \left(\frac{2}{3} - 2C \right) \eta \right], \quad (11)$$

$$\frac{dn_s}{dN} \approx -16\epsilon\eta + 24\epsilon^2 + 2\xi, \quad (12)$$

where the Euler constant $\gamma \approx 0.577$, $C = \ln 2 + \gamma - 2 \approx -0.73$ and

$$\xi = \frac{d\eta}{dN} + 2\epsilon\eta. \quad (13)$$

The observational data requires $n_s - 1 \sim 2/N$, so ϵ and η are at most in the order of $1/N$, their derivatives with respect to N have at most the order of $1/N^2$, so ξ is at most in the order of $1/N^2$. Therefore, the running of the scalar spectral index and the second-order corrections will be in the order of $1/N^2$, we may neglect the second-order corrections.

3 THE PARAMETRIZATION OF THE SPECTRAL TILT

We approximate n_s as

$$n_s - 1 \approx -\frac{p}{N + \alpha}, \quad (14)$$

where the constants p and α are both positive, and the constant α accounts for the contribution from the scalar field ϕ_e at the end of inflation. With this approximation, then n_s

is well behaved at the end of inflation when $N = 0$. Note that the functional form of the potential is not affected by α . The observational results favour $p > 1$, so we consider $p > 1$ only.

For $p > 1$, the solution to Equation (3) is

$$\epsilon(N) = \frac{p-1}{2(N+\alpha) + C(N+\alpha)^p}, \quad (15)$$

where $C \geq 0$ is an integration constant. This is a generalization of the Mukhanov parametrization $\epsilon(N) = \beta/(N+1)^p$ (Mukhanov 2013). Since $\epsilon(N=0) \approx 1$, so $2\alpha + C\alpha^p \approx p-1$. If $C < 0$, then $|C|$ must be a very small number to ensure that $0 < \epsilon(N=60) \ll 1$, and its contribution is negligible so that we can take it to be zero. Therefore, we consider $C \geq 0$ only. Since

$$C \approx \frac{p-1-2\alpha}{\alpha^p}, \quad (16)$$

so $C \geq 0$ requires that $p \geq 2\alpha + 1$.

Combining Equations (2) and (15), we get

$$\eta(N) = \frac{3(p-1)}{2(N+\alpha) + C(N+\alpha)^p} - \frac{p}{2(N+\alpha)}. \quad (17)$$

For $N \gg 1$ and $C \sim 1$, $\epsilon \sim 1/(N+\alpha)^p$ and $\eta \sim -1/(N+\alpha)$, so the tensor to scalar ratio $r \sim 1/(N+\alpha)^p$ is small and only η contributes to n_s .

Either solving Equation (7) with the parametrization (14), or solving Equation (6) with the solution (15), we get (Chiba 2015)

$$V(N) = \frac{p-1}{A} \left[\frac{1}{(N+\alpha)^{p-1}} + \frac{C}{2} \right]^{-1}, \quad (18)$$

where $A > 0$ is an integration constant.

Let us consider the special case $C = 0$ first. For $C = 0$, we get

$$\epsilon(N) = \frac{p-1}{2(N+\alpha)}, \quad (19)$$

and

$$\eta(N) = \frac{2p-3}{2(N+\alpha)}. \quad (20)$$

Therefore, both ϵ and η contribute to the scalar spectral tilt and

$$r = \frac{8(p-1)}{p}(1-n_s). \quad (21)$$

Substituting Equation (19) into Equation (9), we get

$$\phi - \phi_e = \pm 2\sqrt{p-1}(\sqrt{N+\alpha} - \sqrt{\alpha}), \quad (22)$$

or

$$\phi(N) = \pm 2\sqrt{(p-1)(N+\alpha)} + \phi_0, \quad (23)$$

where ϕ_0 is an arbitrary integration constant, and $\phi_e = \pm 2\sqrt{(p-1)\alpha} + \phi_0$. Since $2\alpha \sim p-1$, so $\phi \gtrsim 1$ and this model corresponds to large field inflation. Combining Equations (23) and (18), we get the power-law potential for chaotic inflation (Linde 1983)

$$V(\phi) = \frac{p-1}{A(p-1)^{p-1}} \left(\frac{\phi - \phi_0}{2} \right)^{2(p-1)} = V_0(\phi - \phi_0)^{2(p-1)}. \quad (24)$$

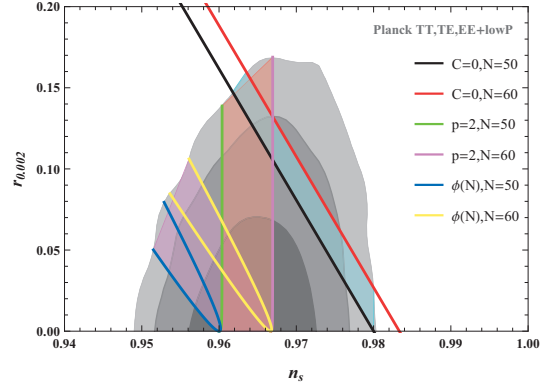


Figure 1. The marginalized 68%, 95% and 99.8% CL contours for n_s and $r_{0.002}$ from Planck 2015 data (Planck Collaboration XX 2015) and the observational constraints on the parametrizations (15) and $\phi(N) = \sigma \ln(\beta N + \gamma)$. The cyan regions are for the parametrization (15) with $C = 0$, the brown regions are for the parametrization (15) with $p = 2$, and the magenta areas are for the parametrization $\phi(N) = \sigma \ln(\beta N + \gamma)$.

For simplicity, we apply the Planck 2015 68% CL constraints on r and n_s to the $r - n_s$ relation (21) (Planck Collaboration XX 2015), and we find that no p satisfies the 68% CL constraints as shown in Fig. 1. At about the 99.8% CL level, $1.00 < p \leq 1.93$ and $0 < \Delta\phi \leq 12.39$ for $N = 50$, $1.20 \leq p \leq 2.21$ and $6.65 \leq \Delta\phi \leq 15.42$ for $N = 60$. From the above analysis, we see that the power-law potential is disfavoured by the observations at the 68% CL, and the field excursion for the inflaton is super-Planckian. For $N = 50$, $p \sim 1$ is marginally consistent with the observational constraint at the 99.8% CL, it is possible that the field excursion of the inflaton is sub-Planckian and the tensor to scalar ratio r is close to zero.

Next we consider the special case with $p = 2$. For this case, we get

$$\phi(N) = \pm \frac{2\sqrt{2}}{\sqrt{C}} \operatorname{arcsinh} \sqrt{C(N+\alpha)/2} + \phi_0, \quad (25)$$

$$\phi_e = \pm \frac{2\sqrt{2}}{\sqrt{C}} \operatorname{arcsinh} \sqrt{C\alpha/2} + \phi_0, \quad (26)$$

where ϕ_0 is an arbitrary integration constant and $C = (1 - 2\alpha)/\alpha^2 > 0$. Combining Equations (25) and (18), we get the corresponding T-model potential (Kallosh & Linde 2013),

$$V(\phi) = \frac{2}{AC} \tanh^2 \left[\frac{\sqrt{C}}{2\sqrt{2}} (\phi - \phi_0) \right] = V_0 \tanh^2 [\gamma(\phi - \phi_0)], \quad (27)$$

where $\gamma = \sqrt{C}/8$. If $C \ll (N+\alpha)^{-1}$ or $\alpha \rightarrow 1/2$, then the potential reduces to the quadratic potential. From the discussion on the power-law potential, we know that the inflaton is a large field and it is disfavoured by the observations at the 68% CL level. If $C > 1$ or $\alpha \ll 1$, then the potential becomes

$$V(\phi) \approx V_0 \left\{ 1 - 2 \exp \left[-\sqrt{C/2} (\phi - \phi_0) \right] \right\}^2 \approx V_0 \left\{ 1 - 4 \exp \left[-\sqrt{C/2} (\phi - \phi_0) \right] \right\}. \quad (28)$$

The potential includes the models with α -attractors (Kallosh et al. 2013) and the Starobinsky model

(Starobinsky 1980) when $C = 4/3$ or $\alpha = (\sqrt{21} - 3)/4$. By fitting Equations (14) and (15) to the Planck 2015 data, for $N = 50$, we get $\alpha < 0.4993$ and $0 < \Delta\phi \leq 13.90$ at the 99.8% CL, for $N = 60$, we get $\alpha < 0.5009$ and $0 < \Delta\phi \leq 15.49$ at the 99.8% CL. The results are shown in Fig. 1. Here we extend the integration constant C to the region of $C < 0$, and we verify the conclusion that $|C|$ is very small if $C < 0$ as discussed above. The above results also tell us that this model can be either small field inflation or large field inflation depending on the value of α . If $\alpha \ll 1$, then $C \gg 1$ and $\Delta\phi$ is small. If α is close to $1/2$, then C is close to zero, and $\Delta\phi$ is large.

For the general case with $C > 0$ and $p \neq 2$, we get

$$\phi(N) = \phi_0 \pm \frac{2}{2-p} \sqrt{\frac{2(p-1)}{C}} (N+\alpha)^{1-p/2} \times {}_2F_1 \left[\frac{1}{2}, \frac{p-2}{2(p-1)}, \frac{4-3p}{2-2p}, -\frac{2(N+\alpha)^{1-p}}{C} \right]. \quad (29)$$

The analytical form of the potential is not apparent, so we analyse the asymptotic form of the potential. For $C \ll 1$, the potential will be the same as the case with $C = 0$, and it is the power-law potential. For $C > 1$, Equation (15) can be approximated as

$$\epsilon(N) \approx \frac{p-1}{C(N+\alpha)^p}, \quad (30)$$

and Equation (29) can be approximated as

$$\phi(N) = \phi_0 \pm \frac{2}{2-p} \sqrt{\frac{2(p-1)\alpha^p}{p-1-2\alpha}} (N+\alpha)^{(2-p)/2}, \quad (31)$$

and

$$\phi_e = \phi_0 \pm \frac{2\alpha}{2-p} \sqrt{\frac{2(p-1)}{p-1-2\alpha}}. \quad (32)$$

Combining Equations (18) and (31), for $C > 1$, the potential is

$$V(\phi) = \frac{2(p-1)\alpha^p}{A(p-1-2\alpha)} \left\{ 1 \mp \left(\frac{2\alpha^p}{p-1-2\alpha} \right)^{1/(2-p)} \times \left[\frac{2-p}{2\sqrt{p-1}} (\phi - \phi_0) \right]^{-2(p-1)/(2-p)} \right\}^{-1}. \quad (33)$$

If $p > 2$, then for small field ϕ , the potential reduces to the hilltop potential $V(\phi) = V_0[1 - (\phi/M)^n]$ (Boubekeur & Lyth 2005) with $n = 2(p-1)/(p-2)$ (Garcia-Bellido & Roest 2014; Creminelli et al. 2015). If $1 < p < 2$, then for large field ϕ , the potential reduces to the form $V(\phi) = V_0[1 - (M/\phi)^n]$ with $n = 2(p-1)/(2-p)$ (Garcia-Bellido & Roest 2014; Creminelli et al. 2015). Fitting the model with general p and α to the observational data (Planck Collaboration XX 2015), we find the constraints on p and α for $N = 60$ and the results are shown in Fig. 2. The results tell us that the model can accommodate both small and large field inflation. Because $p > 2\alpha + 1$, so the parametrization (14) requires that $(1-n_s)(N+\alpha) > 2\alpha + 1$. At the 99.8% CL, $0.02 \lesssim n_s \lesssim 0.05$, so $\alpha \lesssim 1.03$ and $1.18 < p < 3.11$ if we take $N = 60$.

4 THE PARAMETRIZATION OF $\epsilon(N)$

For the parametrization

$$\epsilon(N) = \frac{\alpha}{1 + s \exp(-\beta N)}, \quad (34)$$

we get

$$n_s - 1 = \frac{-2\alpha + \beta s \exp(-\beta N)}{1 + s \exp(-\beta N)}. \quad (35)$$

Note that for the parametrization in this section, we take $s = \pm 1$ for simplicity, $\alpha > 0$, $\beta > 0$ and the parameter $N = N_* + N_e$ so that we consider the contribution from ϕ_e , i.e., at the end of inflation, $0 < N = N_e \ll N_*$. When $s = -1$, we require $\exp(\beta N_e) > 1$. Substitute the parametrization (34) into Equation (6), we get

$$V(N) = V_0 [s + \exp(\beta N)]^{2\alpha/\beta}. \quad (36)$$

Using Equation (8), we get

$$\phi(N) = \phi_0 \pm \frac{2\sqrt{2\alpha}}{\beta} \ln \left[\exp(\beta N/2) + \sqrt{s + \exp(\beta N)} \right], \quad (37)$$

and

$$\phi_e = \phi_0 \pm \frac{2\sqrt{2\alpha}}{\beta} \ln \left[\exp(\beta N_e/2) + \sqrt{s + \exp(\beta N_e)} \right]. \quad (38)$$

Combining Equations (36) and (37), we get

$$V(\phi) = V_0 \left[s + \left(\frac{U(\phi) - sU^{-1}(\phi)}{2} \right)^2 \right]^{2\alpha/\beta}, \quad (39)$$

where $U(\phi) = \exp(\pm\beta(\phi - \phi_0)/(2\sqrt{2\alpha}))$. For $s = 1$, the potential is

$$V(\phi) = V_0 \left[\cosh \left(\frac{\beta(\phi - \phi_0)}{2\sqrt{2\alpha}} \right) \right]^{4\alpha/\beta}. \quad (40)$$

By fitting Equations (34) and (35) with $s = 1$ to the Planck 2015 data (Planck Collaboration XX 2015), we find that α and β satisfies the 99.8% CL constraints.

For $s = -1$, the potential is

$$V(\phi) = V_0 \left[\sinh \left(\frac{\beta(\phi - \phi_0)}{2\sqrt{2\alpha}} \right) \right]^{4\alpha/\beta}. \quad (41)$$

Fitting Equations (34) and (35) with $s = -1$ to the Planck 2015 data (Planck Collaboration XX 2015), we find that α and β satisfies the 68% CL constraints, so the model is disfavoured at the 68% CL. The 95% and 99.8% CL constraints on α and β for $N = 60$ are shown in Fig. 3. By using the 99.8% CL constraints, we find that $8.37 \leq \Delta\phi \leq 16.48$, so the field excursion of the inflaton in this model is super-Planckian.

For the parametrization

$$\epsilon(N) = \frac{\alpha \exp(-\beta N)}{1 + s \exp(-\beta N)}, \quad (42)$$

we get

$$n_s - 1 = -\frac{\beta + 2\alpha \exp(-\beta N)}{1 + s \exp(-\beta N)}. \quad (43)$$

Substitute the parametrization (42) into Equation (6), we get

$$V(N) = V_0 [1 + s \exp(-\beta N)]^{-2\alpha/(\beta s)}. \quad (44)$$

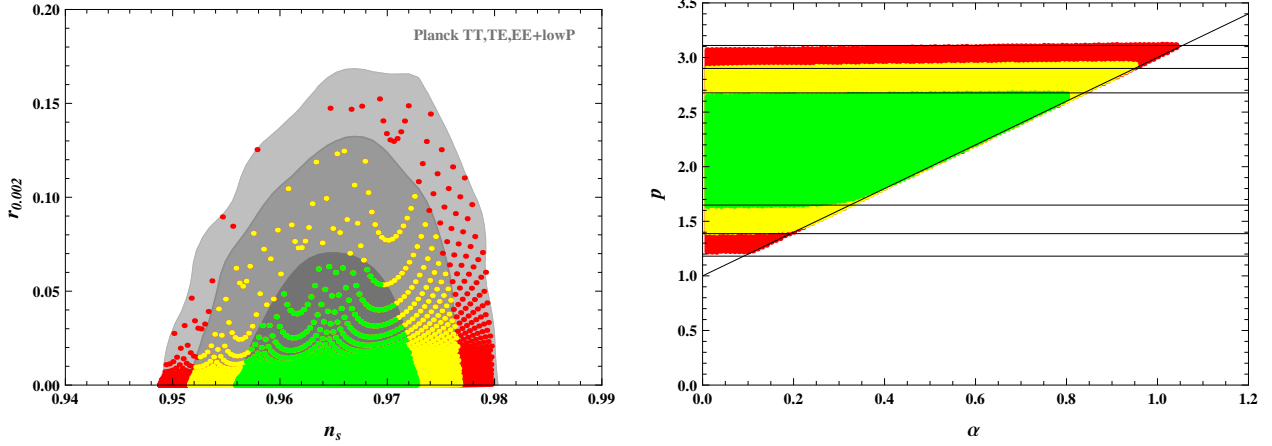


Figure 2. The marginalized 68%, 95% and 99.8% CL contours for n_s and $r_{0.002}$ from Planck 2015 data (Planck Collaboration XX 2015) and the observational constraints on the parametrization (15). The left-hand panel shows the $n_s - r$ contours and the right-hand panel shows the constraints on p and α for $N = 60$. The green, yellow and red regions correspond to 68%, 95% and 99.8% CLs, respectively.

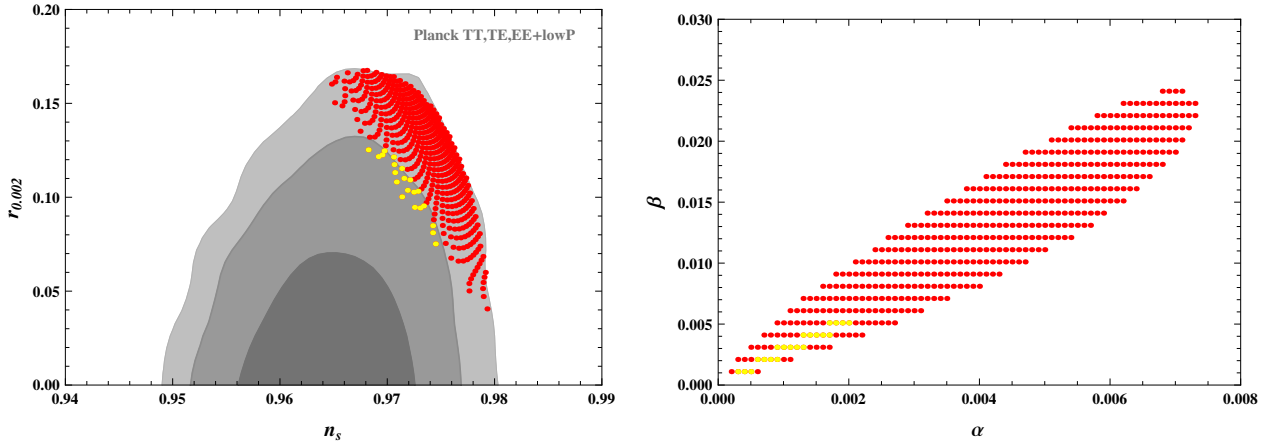


Figure 3. The marginalized 68%, 95% and 99.8% CL contours for n_s and $r_{0.002}$ from Planck 2015 data (Planck Collaboration XX 2015) and the observational constraints on the parametrizations (34) with $s = -1$. The left-hand panel shows the $n_s - r$ contours and the right-hand panel shows the constraints on α and β for $N = 60$. The yellow and red regions correspond to 95% and 99.8% CLs, respectively.

From Equation (8), we get

$$\phi(N) = \phi_0 \mp \frac{2\sqrt{2\alpha}}{\beta\sqrt{s}} \operatorname{arcoth} \left[\sqrt{\frac{s + \exp(\beta N)}{s}} \right]. \quad (45)$$

For $s = 1$, we get

$$\phi_e = \phi_0 \mp \frac{2\sqrt{2\alpha}}{\beta} \operatorname{arcoth} \left[\sqrt{1 + \exp(\beta N_e)} \right], \quad (46)$$

and the potential

$$V(\phi) = V_0 \left[\operatorname{sech} \left(\frac{\beta(\phi - \phi_0)}{2\sqrt{2\alpha}} \right) \right]^{4\alpha/\beta}. \quad (47)$$

If $\beta = 4\alpha = 2/M^2$, we recover the potential for the s-dual inflation $V = V_0 \operatorname{sech}(\phi/M)$ (Anchordoqui et al. 2014). Fitting Equations (42) and (43) with $s = 1$ to the Planck 2015 data (Planck Collaboration XX 2015), we obtain the constraints on the parameters α and β for $N = 60$ and the results are shown in Fig. 4. From Fig. 4, we see that the s-dual inflation is consistent with the observational data. By using the 99.8% CL constraints, we find that $0 < \Delta\phi \leq 26.57$, so the

model includes both the large field and small field inflation. If α is close to zero, then $\Delta\phi$ is small.

For $s = -1$, we get the potential,

$$V(\phi) = V_0 \left[\sin \left(\frac{\beta(\phi - \phi_0)}{2\sqrt{2\alpha}} \right) \right]^{4\alpha/\beta}, \quad (48)$$

or

$$\begin{aligned} V(\phi) &= V_0 \left[\cos \left(\frac{\beta(\phi - \phi_0)}{2\sqrt{2\alpha}} \right) \right]^{4\alpha/\beta} \\ &= \frac{V_0}{4} \left[1 + \cos \left(\frac{\beta(\phi - \phi_0)}{\sqrt{2\alpha}} \right) \right]^{2\alpha/\beta}, \end{aligned} \quad (49)$$

If we take $\beta = 2\alpha$ and $f = 1/\sqrt{2\alpha}$, then we recover the potential for natural inflation $V(\phi) = \Lambda^4 [1 + \cos(\phi/f)]$ (Freese et al. 1990). Fitting Equations (42) and (43) with $s = -1$ to the Planck 2015 data (Planck Collaboration XX 2015), we obtain the constraints on the parameters α and β for $N = 60$ and the results are shown in Fig. 5. From Fig. 5, we see that natural inflation is disfavoured at the 68% CL. By using the 99.8% CL constraints, we find that

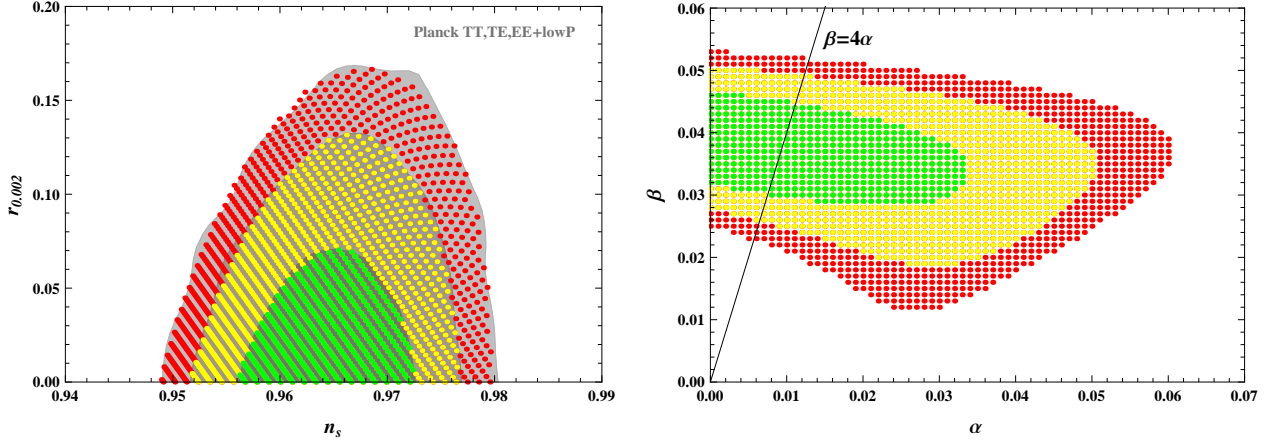


Figure 4. The marginalized 68%, 95% and 99.8% CL contours for n_s and $r_{0.002}$ from Planck 2015 data (Planck Collaboration XX 2015) and the observational constraints on the parametrizations (42) with $s = 1$. The left-hand panel shows the $n_s - r$ contours and the right-hand panel shows the constraints on α and β for $N = 60$. The green, yellow and red regions correspond to 68%, 95% and 99.8% CLs, respectively. The solid line $\beta = 4\alpha$ in the right-hand panel corresponds to the s -dual inflation.

$0 < \Delta\phi \leq 54.41$, so the model includes both the large field and small field inflation, and the small field inflation is achieved when α is close to zero.

For the parametrization

$$\epsilon(N) = \frac{\alpha \exp(-\beta N)}{[1 + s \exp(-\beta N)]^2}, \quad (50)$$

we get

$$n_s - 1 = \frac{-\beta - 2\alpha \exp(-\beta N) + \beta s^2 \exp(-2\beta N)}{[1 + s \exp(-\beta N)]^2}, \quad (51)$$

$$V(N) = V_0 \exp \left[\frac{-2\alpha}{\beta[s + \exp(\beta N)]} \right], \quad (52)$$

and

$$\phi(N) = \phi_0 \pm \frac{2\sqrt{2\alpha}}{\beta\sqrt{s}} \arctan [\exp(\beta N/2)/\sqrt{s}]. \quad (53)$$

For $s = -1$, we get the potential

$$V(\phi) = V_0 \exp \left[-\frac{2\alpha}{\beta} \sinh^2 \left(\frac{\beta(\phi - \phi_0)}{2\sqrt{2\alpha}} \right) \right]. \quad (54)$$

If $\beta = 2\alpha = 4/\mu^2$, then the potential reduces to the hilltop potential $V(\phi) = V_0[1 - (\phi/\mu)^p]$ with $p = 2$ for small ϕ . If $\alpha = \beta = 8/\mu^2$, then the potential reduces to the double well potential $V(\phi) = V_0[1 - (\phi/\mu)^2]^2$ for small ϕ (Olive 1990). Fitting Equations (50) and (51) with $s = -1$ to the Planck 2015 data (Planck Collaboration XX 2015), we obtain the constraints on the parameters α and β for $N = 60$ and the results are shown in Fig. 6. From Fig. 6, we see that the double well potential is excluded by the observational data and the hilltop potential with $p = 2$ is disfavoured at the 68% CL. By using the 99.8% CL constraints, we find that $0 < \Delta\phi \leq 14.31$, so the model includes both the large field and small field inflation. If α is close to zero, then $\Delta\phi$ is small.

For $s = 1$, we get the potential

$$V(\phi) = V_0 \exp \left[-\frac{\alpha}{\beta} \left(1 + \cos \frac{\beta(\phi - \phi_0)}{\sqrt{2\alpha}} \right) \right]. \quad (55)$$

Fitting Equations (50) and (51) with $s = 1$ to the Planck

2015 data (Planck Collaboration XX 2015), we obtain the constraints on the parameters α and β for $N = 60$ and the results are shown in Fig. 7. By using the 99.8% CL constraints, we find that $0 < \Delta\phi \leq 31.23$, so the model includes both the large field and small field inflation, and the small field inflation is achieved if α is close to zero.

5 THE PARAMETRIZATION OF $\phi(N)$

Combining Equations (6) and (8), we get

$$(\ln V)_{,N} = (\phi_{,N})^2. \quad (56)$$

Once the functional form $\phi(N)$ is known, we can derive the potential form $V(\phi)$. Let us first consider the power-law parametrization

$$\phi(N) = \sigma(N + \gamma)^\beta. \quad (57)$$

For $\beta = 1/2$, from Equation (56), we get the power-law potential,

$$V(\phi) = V_0(N + \gamma)^{\frac{\sigma^2}{4}} = V_0 \left(\frac{\phi}{\sigma} \right)^{\frac{\sigma^2}{2}}, \quad (58)$$

where V_0 is an integration constant. From Equation (8), we get

$$\epsilon = \frac{\sigma^2}{8(N + \gamma)}, \quad (59)$$

so

$$n_s - 1 = -\frac{1 + \sigma^2/4}{N + \gamma}, \quad r = \frac{2\sigma^2}{N + \gamma}, \quad (60)$$

and $\sigma^2 \approx 8\gamma$. The results are the same as those discussed in Section 3 with $C = 0$, $p = 1 + \sigma^2/4$ and $\alpha = \gamma$.

For $\beta \neq 1/2$, we derive the potential,

$$\begin{aligned} V(\phi) &= V_0 \exp \left[\frac{\sigma^2 \beta^2}{2\beta - 1} (N + \gamma)^{2\beta - 1} \right] \\ &= V_0 \exp \left[\frac{\sigma^2 \beta^2}{2\beta - 1} \left(\frac{\phi}{\sigma} \right)^{2 - 1/\beta} \right], \end{aligned} \quad (61)$$

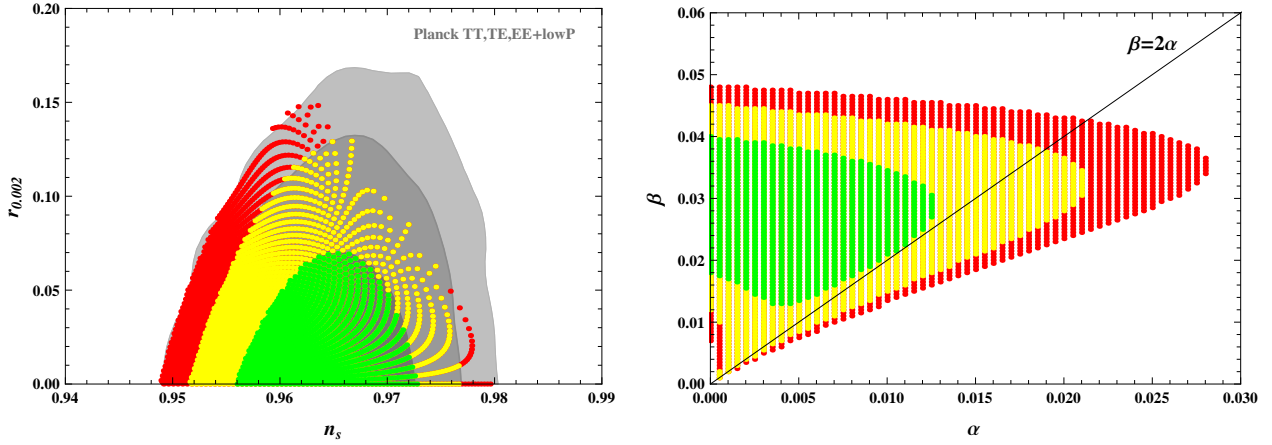


Figure 5. The marginalized 68%, 95% and 99.8% CL contours for n_s and $r_{0.002}$ from Planck 2015 data (Planck Collaboration XX 2015) and the observational constraints on the parametrizations (42) with $s = -1$. The left-hand panel shows the $n_s - r$ contours and the right-hand panel shows the constraints on α and β for $N = 60$. The green, yellow and red regions correspond to 68%, 95% and 99.8% CLs, respectively. The solid line $\beta = 2\alpha$ in the right-hand panel corresponds to the natural inflation.

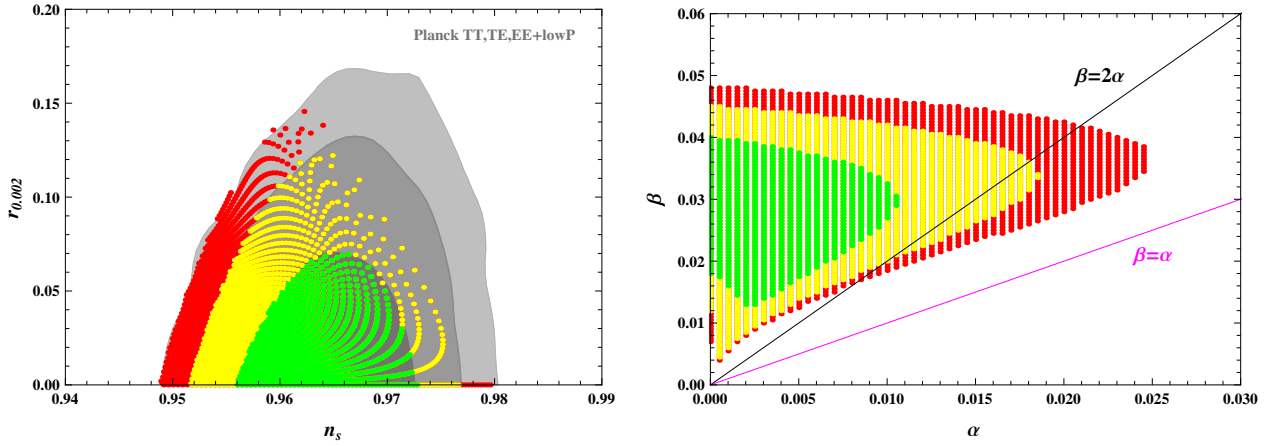


Figure 6. The marginalized 68%, 95% and 99.8% CL contours for n_s and $r_{0.002}$ from Planck 2015 data (Planck Collaboration XX 2015) and the observational constraints on the parametrizations (50) with $s = -1$. The left-hand panel shows the $n_s - r$ contours and the right-hand panel shows the constraints on α and β for $N = 60$. The green, yellow and red regions correspond to 68%, 95% and 99.8% CLs, respectively. The black solid line $\beta = 2\alpha$ in the right-hand panel corresponds to the hilltop potential with $p = 2$, and the magenta solid line $\beta = \alpha$ corresponds to the double well potential.

the scalar spectral tilt,

$$n_s - 1 = \frac{2\beta - 2}{N + \gamma} - \sigma^2 \beta^2 (N + \gamma)^{2\beta - 2}, \quad (62)$$

the tensor to scalar ratio,

$$r = 8\sigma^2 \beta^2 (N + \gamma)^{2\beta - 2}, \quad (63)$$

and the parameters σ , β and γ satisfy the relation $\sigma^2 \beta^2 \approx 2\gamma^{2-2\beta}$. Note that Equations (62) and (63) include the special case $\beta = 1/2$ which corresponds to the power-law potential. Fitting Equations (62) and (63) for the parametrization (57) to the Planck 2015 data (Planck Collaboration XX 2015), we obtain the constraints on the parameters α and β for $N = 60$ and the results are shown in Fig. 8. By using the 99.8% CL constraints, we find that $0 < \Delta\phi \leq 754.23$. If β is near zero, then it is large field inflation. If γ is near zero, then it is small field inflation. In the left-hand panel of Fig. 8, the lower bounds of the $n_s - r$ contours are set by $\beta = 0$.

Next we consider the parametrization $\phi(N) =$

$\sigma \ln(\beta N + \gamma)$. Combining Equations (1), (3), (8) and (56), we get

$$\begin{aligned} V(\phi) &= V_0 \exp\left(-\frac{\sigma^2 \beta}{\beta N + \gamma}\right) \\ &= V_0 \exp[-\sigma^2 \beta \exp(-\phi/\sigma)], \end{aligned} \quad (64)$$

$$\epsilon(N) = \frac{\sigma^2 \beta^2}{2(\beta N + \gamma)^2}, \quad (65)$$

$$n_s - 1 = -\frac{2}{N + \gamma/\beta} - \frac{\sigma^2}{(N + \gamma/\beta)^2}, \quad (66)$$

$$r = \frac{8\sigma^2}{(N + \gamma/\beta)^2}. \quad (67)$$

From the end of inflation condition $\epsilon(N = 0) \approx 1$, we get $\sigma^2 \beta^2 = 2\gamma^2$, so $r = 16(\gamma/\beta)^2/(N + \gamma/\beta)^2$, and n_s and r depend on the parameter γ/β only. If γ/β is small, then $n_s - 1 \sim -2/N$ and $r \sim 1/N^2$, and the model will behave like the model (14) with $p = 2$ and small $\alpha = \gamma/\beta$, so the

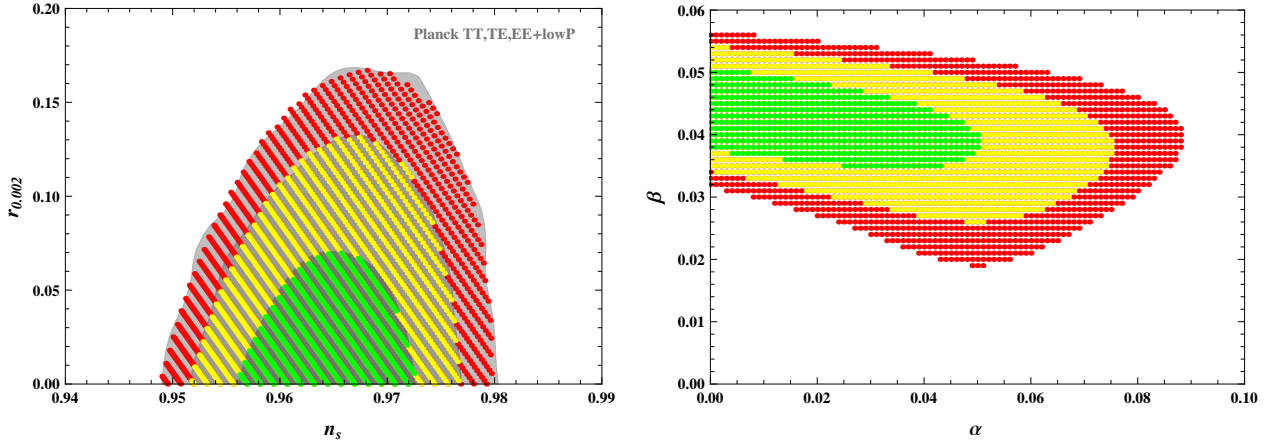


Figure 7. The marginalized 68%, 95% and 99.8% CL contours for n_s and $r_{0.002}$ from Planck 2015 data (Planck Collaboration XX 2015) and the observational constraints on the parametrizations (50) with $s = 1$. The left-hand panel shows the $n_s - r$ contours and the right-hand panel shows the constraints on α and β for $N = 60$. The green, yellow and red regions correspond to 68%, 95% and 99.8% CLs, respectively.

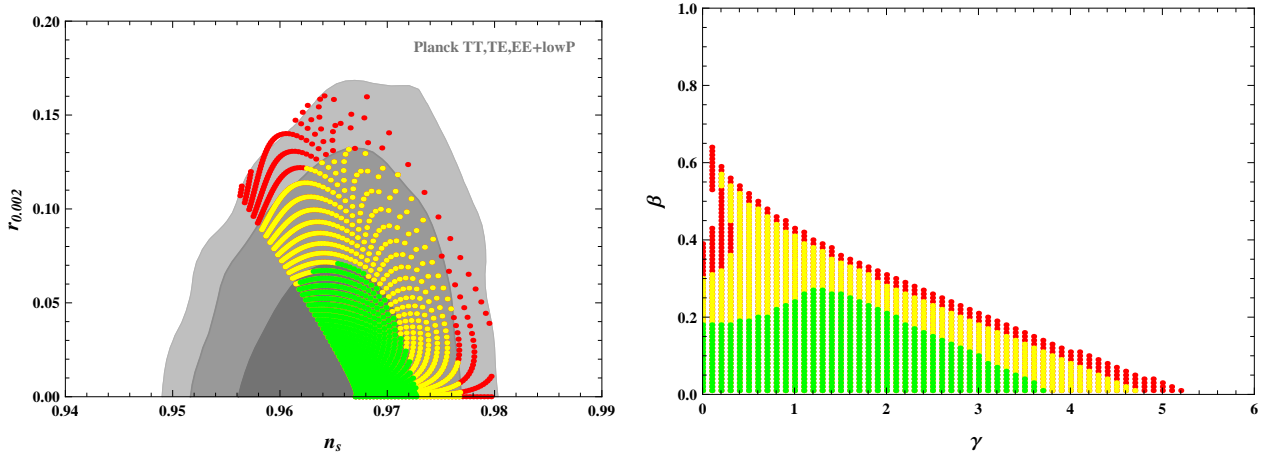


Figure 8. The marginalized 68%, 95% and 99.8% CL contours for n_s and $r_{0.002}$ from Planck 2015 data (Planck Collaboration XX 2015) and the observational constraints on the parametrizations (57). The left-hand panel shows the $n_s - r$ contours and the right-hand panel shows the constraints on β and γ for $N = 60$. The green, yellow and red regions correspond to 68%, 95% and 99.8% CLs, respectively.

two models will cover some common regions in the $n_s - r$ graph. The fitting results are shown in Fig. 1. In particular, for $\phi/\sigma \gg 1$, the potential can be approximated as

$$\begin{aligned} V(\phi) &\approx V_0 [1 - 2\gamma^2 \exp(-\phi/\sigma)] \\ &\approx V_0 [1 - \gamma^2 \exp(-\phi/\sigma)]^2. \end{aligned} \quad (68)$$

Therefore, the R^2 inflation is also included in this model.

In the last we consider the exponential parametrization $\phi(N) = \sigma \exp(\beta N + \gamma)$ with $\beta < 0$. Following the same procedure as above, we obtain

$$V(\phi) = V_0 \exp(\beta\phi^2/2), \quad (69)$$

$$\epsilon = \frac{\sigma^2 \beta^2}{2} \exp(2\beta N + 2\gamma) = r/16, \quad (70)$$

$$n_s - 1 = 2\beta - \beta^2 \sigma^2 \exp(2\beta N + 2\gamma). \quad (71)$$

The model parameters satisfy the relation $\beta^2 \sigma^2 \exp(2\gamma) = 2$, so $\epsilon = \exp(\beta N)$ and $n_s - 1 = 2\beta - 2\exp(2\beta N)$. Since $\epsilon < 1$, the parameter β should be negative. From the constraint on r , we can get the upper limit on β , with this upper limit, we

find that the model is not consistent with the observational data.

6 CONCLUSIONS

For the double well potential $V(\phi) = V_0[1 - (\phi/\mu)^2]^2$, the potential $V(\phi) = V_0 \exp(\beta\phi^2)$ and the potential $V(\phi) = V_0[\cosh(\beta\phi/2\sqrt{2\alpha})]^{4\alpha/\beta}$, the predicted n_s and r are not consistent with the Planck 2015 data. The power-law potential $V(\phi) = V_0\phi^{2p-2}$, the potential $V(\phi) = V_0[\sinh(\beta\phi/2\sqrt{2\alpha})]^{4\alpha/\beta}$, the natural inflation and the hill-top potential with $n = 2$ are disfavoured by the observational data at the 68% CL. At the 99.8% CL, we find that $1.2 \leq p \leq 2.21$ for the power-law potential if we take the number of e-folds before the end of inflation $N = 60$. For the power-law potential $V(\phi) = V_0(\phi - \phi_0)^{2(p-1)}$, the T-model potential $V(\phi) = V_0 \tanh^2(\gamma\phi)$ which includes the α -attractors and the Starobinsky model, the hilltop potential $V(\phi) = V_0[1 - (\phi/M)^n]$ with $n = 2(p-1)/(p-2)$

and $p > 2$, the potential $V(\phi) = V_0[1 - (M/\phi)^n]$ with $n = 2(p - 1)/(2 - p)$ and $1 < p < 2$, and the potential $V(\phi) = V_0 \exp[-\sigma^2 \beta \exp(-\phi/\sigma)]$, their spectral tilts have the universal behavior $n_s = -p/(N + \alpha)$.

For the parametrization $\epsilon(N) = \alpha \exp(-\beta N)/[1 + \exp(-\beta N)]$, we get $n_s - 1 = -[\beta + 2\alpha \exp(-\beta N)]/[1 + \exp(-\beta N)]$ and the corresponding potential $V(\phi) = V_0[\text{sech}(\beta\phi/2\sqrt{2\alpha})]^{4\alpha/\beta}$ which includes the s-dual inflation. For the parametrization $\epsilon(N) = \alpha \exp(-\beta N)/[1 - \exp(-\beta N)]$, we get $n_s - 1 = -[\beta + 2\alpha \exp(-\beta N)]/[1 - \exp(-\beta N)]$ and the corresponding potential $V(\phi) = V_0[\text{sinh}(\beta\phi/2\sqrt{2\alpha})]^{4\alpha/\beta}$ which includes the natural inflation. For the parametrization $\epsilon(N) = \alpha \exp(-\beta N)/[1 - \exp(-\beta N)]^2$, we get the corresponding potential $V(\phi) = V_0 \exp[-2\alpha \sinh^2(\beta\phi/2\sqrt{2\alpha})/\beta]$ which includes the hilltop potential with $n = 2$ and the double well potential. The tensor to scalar ratio r for these models can easily be small due to the factor $\exp(-\beta N)$ in $\epsilon(N)$. For the parametrization $\phi(N) = \sigma \ln(\beta N + \gamma)$, the corresponding potential is $V(\phi) = V_0 \exp[-\sigma^2 \beta \exp(-\phi/\sigma)]$, both n_s and r depend on γ/β only and the model has the universal behavior $n_s - 1 = -2/(N + \gamma/\beta)$ if γ/β is small. All these models can achieve both small and large field inflation.

Based on the slow-roll relations (3), (6), (7) and (8), by parameterizing one of the parameters $n_s(N)$, $\epsilon(N)$ and $\phi(N)$, and fitting the parameters in the models to the observational data, we not only obtain the constraints on the parameters, but also easily reconstruct the classes of the inflationary models which include the chaotic inflation, T-model, hilltop inflation, s-dual inflation, natural inflation and R^2 inflation, and the reconstructed inflationary models are consistent with the observations. Since the observational data only probes a rather small intervals of scales, the reconstructed potentials approximate the inflationary potential only in the slow-roll regime for the observational scales $10^{-3} \text{ Mpc} \lesssim k^{-1} \lesssim 10^4 \text{ Mpc}$. Outside the slow-roll regime, the inflationary potential can be rather different, but it does not mean that the reconstructed potential is not applicable in that regime. Once the potential is obtained, we can either apply the slow-roll formulae or work out the exact solutions.

ACKNOWLEDGEMENTS

This research was supported in part by the Natural Science Foundation of China under Grants Nos. 11175270 and 11475065, and the Program for New Century Excellent Talents in University under Grant No. NCET-12-0205.

REFERENCES

- Anchordoqui L. A., Barger V., Goldberg H., Huang X., Marfatia D., 2014, *Phys. Lett. B*, 734, 134
 Barranco L., Boubekeur L., Mena O., 2014, *Phys. Rev. D*, 90, 063007
 Boubekeur L., Lyth D., 2005, *J. Cosmol. Astropart. Phys.*, 0507, 010
 Boubekeur L., Giusarma E., Mena O., Ramírez H., 2015, *Phys. Rev. D*, 91, 083006
 Chiba T., 2015, *Prog. Theor. Exp. Phys.*, 2015, 073E02
 Choudhury S., 2015, *Nucl. Phys. B*, 894, 29
 Choudhury S., 2016, *Phys. Dark Univ.*, 11, 16

- Choudhury S., Mazumdar A., 2014a, arXiv: 1403.5549 ([arXiv:1403.5549](#))
 Choudhury S., Mazumdar A., 2014b, *Nucl. Phys. B*, 882, 386
 Copeland E. J., Kolb E. W., Liddle A. R., Lidsey J. E., 1993, *Phys. Rev. D*, 48, 2529
 Creminelli P., Dubovsky S., López Nacir D., Simonović M., Trevisan G., Villadoro G., Zaldarriaga M., 2015, *Phys. Rev. D*, 92, 123528
 Freese K., Frieman J. A., Olinto A. V., 1990, *Phys. Rev. Lett.*, 65, 3233
 Gao Q., Gong Y., 2014, *Phys. Lett. B*, 734, 41
 Gao Q., Gong Y., Li T., Tian Y., 2014, *Sci. China Phys. Mech. Astron.*, 57, 1442
 Gao Q., Gong Y., Li T., 2015, *Phys. Rev. D*, 91, 063509
 Garcia-Bellido J., Roest D., 2014, *Phys. Rev. D*, 89, 103527
 Gobetti R., Pajer E., Roest D., 2015, *J. Cosmol. Astropart. Phys.*, 1509, 058
 Hodges H. M., Blumenthal G. R., 1990, *Phys. Rev. D*, 42, 3329
 Kallosh R., Linde A., 2013, *J. Cosmol. Astropart. Phys.*, 1307, 002
 Kallosh R., Linde A., Roest D., 2013, *J. High Energy Phys.*, 1311, 198
 Kallosh R., Linde A., Roest D., 2014, *Phys. Rev. Lett.*, 112, 011303
 Liddle A. R., Turner M. S., 1994, *Phys. Rev. D*, 50, 758
 Lidsey J. E., Liddle A. R., Kolb E. W., Copeland E. J., Barreiro T., et al., 1997, *Rev. Mod. Phys.*, 69, 373
 Linde A. D., 1983, *Phys. Lett. B*, 129, 177
 Ma Y.-Z., Wang Y., 2014, *J. Cosmol. Astropart. Phys.*, 1409, 041
 Martin J., Ringeval C., Vennin V., 2014a, *Phys. Dark Univ.*, 5-6, 75
 Martin J., Ringeval C., Trozza R., Vennin V., 2014b, *J. Cosmol. Astropart. Phys.*, 1403, 039
 Mukhanov V., 2013, *Eur. Phys. J. C*, 73, 2486
 Mukhanov V. F., Chibisov G. V., 1981, *J. Exp. Theor. Phys. Lett.*, 33, 532
 Myrzakulov R., Sebastiani L., Zerbini S., 2015, *Eur. Phys. J. C*, 75, 215
 Norena J., Wagner C., Verde L., Peiris H. V., Easther R., 2012, *Phys. Rev. D*, 86, 023505
 Olive K. A., 1990, *Phys. Rep.*, 190, 307
 Peiris H., Easther R., 2006, *J. Cosmol. Astropart. Phys.*, 0607, 002
 Planck Collaboration I., 2015, preprint ([arXiv:1502.01582](#))
 Planck Collaboration XX., 2015, preprint ([arXiv:1502.02114](#))
 Roest D., 2014, *J. Cosmol. Astropart. Phys.*, 1401, 007
 Schwarz D. J., Terrero-Escalante C. A., Garcia A. A., 2001, *Phys. Lett. B*, 517, 243
 Starobinsky A. A., 1979, *J. Exp. Theor. Phys. Lett.*, 30, 682
 Starobinsky A. A., 1980, *Phys. Lett. B*, 91, 99
 Stewart E. D., Lyth D. H., 1993, *Phys. Lett. B*, 302, 171